Heat Mass Transfer (2006) 42: 1017–1023
DOI 10.1007/s00231-005-0068-4

ORIGINAL

W. A. Khan · J. R. Culham · M. M. Yovanovich

Analytical study of heat transfer from circular cylinder in liquid metals

Received: 1 December 2004 / Accepted: 24 November 2005 / Published online: 6 January 2006

Abstract In this study the influence of a thin hydrodynamic boundary layer on the heat transfer from a single circular cylinder in liquid metals having low Prandtl number (0.004–0.03) is investigated under isothermal and isoflux boundary conditions. Two separate analytical heat transfer models, viscous and inviscid, are developed to clarify the discrepancy between previous results. For both models, integral approach of the boundary layer analysis is employed to derive closed form expressions for the calculation of the average heat transfer coefficients. For an inviscid model, the energy equation is solved using potential flow velocity only whereas for a viscous model, a fourth-order velocity profile is used in the hydrodynamic boundary layer and potential flow velocity is used outside the boundary layer. The third-order temperature profile is used inside the thermal boundary layer for both models. It is shown that the inviscid model gives higher heat transfer coefficients whereas viscous flow model gives heat transfer results in a fairly good agreement with the previous experimental/numerical results.

List of Symbols

c_p	specific heat of fluid [J/kg·K]
D	diameter of circular cylinder [m]
h	average heat transfer coefficient [W/m^2·K]
k	thermal conductivity [W/m·K]
Nu_D	Nusselt number based on diameter $\equiv Dh/k_f$
Pe_D	Peclet number based on diameter $\equiv Re_D Pr$
q	heat flux [W/m^2]
Re_D	Reynolds number based on diameter $\equiv D\,U_{app}/v$
s	distance along curved surface of cylinder measured from forward stagnation point [m]
T	temperature [°C]
U_{app}	approach velocity [m/s]
$U(s)$	velocity in inviscid region just outside boundary layer [m/s]
UWF	uniform wall flux
UWT	uniform wall temperature
u	s - component of velocity in boundary layer [m/s]
v	η - component of velocity in boundary layer [m/s]
x, y	Cartesian coordinates

Greek Symbols

α	thermal diffusivity [m^2/s]
Δ	thermal boundary-layer thickness [m]
δ	hydrodynamic boundary-layer thickness [m]
δ_T	thermal boundary layer thickness [m]
η	distance normal to and measured from surface of elliptical cylinder [m]
λ	pressure gradient parameter
v	kinematic viscosity of fluid [m^2/s]
ρ	fluid density [kg/m^3]
θ	angle measured from stagnation point [radians]
ζ	ratio of hydrodynamic to thermal boundary layer thickness $\equiv \delta/\delta_T$

Subscripts

a	ambient
f	fluid
H	hydrodynamic
s	separation
T	thermal
w	wall

W. A. Khan (✉) · J. R. Culham · M. M. Yovanovich
Microelectronics Heat Transfer Laboratory,
Department of Mechanical Engineering,
University of Waterloo, Waterloo, ON N2L 3G1, Canada
E-mail: wkhan@mhtlab.uwaterloo.ca

1 Introduction

The use of liquid metals as a "thermal medium" in nuclear reactor and power-generating systems is increasing day by day due to their excellent heat transfer characteristics. A number of theoretical and experimental investigations to determine the heat transfer character-

istics of liquid metals have been conducted by many researchers; but most of them have been confined to internal flow and very few considered the external boundary layer problem.

To the author's knowledge, the first analytical study of heat transfer to liquid metals across circular cylinders is that of Grosh and Cess [1]. They assumed a potential flow model and used it to determine the heat transfer coefficients of liquid metals for flow across flat plates and normal to cylinders of various cross-sections. They derived theoretical expressions for the average Nusselt numbers for different surface temperature profiles. Later Cess and Grosh [2] applied the same technique for tube banks. There have been only four experimental/numerical studies, Andreevskii [3], Ishiguro et al. [4], Sugiyama and Ishiguro [5]; Ishiguro et al. [6]). Andreevskii [3] investigated experimentally the local and average heat transfer coefficients for flow of liquid sodium normal to a single cylinder. He observed a monotonous decrease in the local heat transfer coefficients from the forward to the rear stagnation points. Ishiguro et al. [4] performed experimental studies to investigate the heat transfer characteristics of liquid sodium flowing uniformly across a circular cylinder. They covered the range of Reynolds numbers from 1200 to 11000 and Prandtl numbers of 0.0058 and 0.0073. They determined local and average Nusselt numbers and found that the assumption of potential flow was inadequate to predict accurately the heat transfer rate. Sugiyama and Ishiguro [5] performed a numerical analysis to support the validity of experimental results of Ishiguro et al. [4]. They applied an inviscid flow model taking account of the separation region and found that the local Nusselt numbers have almost constant values in the separation region. They found good agreement with previous experimental results of Ishiguro et al. [4]. Later Ishiguro et al. [6] extended the range of Reynolds numbers and measured local and average heat transfer rates. They found a considerable discrepancy between their experimental results and the analytical predictions of Grosh and Cess [1], but they comment on the accuracy of their experimental results.

In these analytical studies, the effects of thin hydrodynamic boundary layer were neglected and the heat transfer calculations were based on the assumption of an inviscid flow field only. Although, in liquid metals, the thickness of thermal boundary layer is much greater than the thickness of the hydrodynamic boundary layer, the effects of the thin hydrodynamic boundary layer on the heat transfer process cannot be neglected. In this study, the effects of thin boundary later are taken into account in the viscous model and expressions for the local and average heat transfer coefficients are derived using the energy integral equation.

2 Analysis

Consider a uniform flow of a liquid metal with low Prandtl number past a fixed circular cylinder of diameter D, with vanishing circulation around it, as shown in Fig. 1. The approaching velocity of the fluid is U_{app} and the ambient temperature is assumed to be T_{a}. The surface temperature of the cylinder wall is T_{w} ($> T_{\text{a}}$) in the case of the isothermal cylinder and the heat flux is q for the isoflux boundary condition. The flow is assumed to be laminar, steady, and two-dimensional.

Khan [7] set up the energy equation in a curvilinear system of coordinates in which s denotes distance along the curved surface of the circular cylinder measured from the forward stagnation point A and η is the distance normal to and measured from the surface as shown in Fig. 1. In this system of coordinates, the velocity components are denoted by u and v in the local s- and η-directions. The potential flow velocity just outside the boundary layer is denoted by $U(s)$. Therefore, the energy equation in the curvilinear system is

$$u\frac{\partial T}{\partial s}+v\frac{\partial T}{\partial \eta}=\alpha\frac{\partial^2 T}{\partial \eta^2} \tag{1}$$

3 Thermal boundary conditions

The boundary conditions for the isothermal and isoflux cylinders are as follows.
At the cylinder surface

$$\eta=0,\quad \begin{cases} T=T_{\text{w}} & \text{for UWT} \\ \dfrac{\partial T}{\partial \eta}=-\dfrac{q}{k_{\text{f}}} & \text{for UWF} \end{cases} \tag{2}$$

At the edge of the boundary layer

$$\eta=\delta_{\text{T}},\ T=T_{\text{a}} \text{ and } \frac{\partial T}{\partial \eta}=0 \tag{3}$$

4 Velocity distribution

For the viscous flow model, the velocity distribution in the thin hydrodynamic boundary layer can be

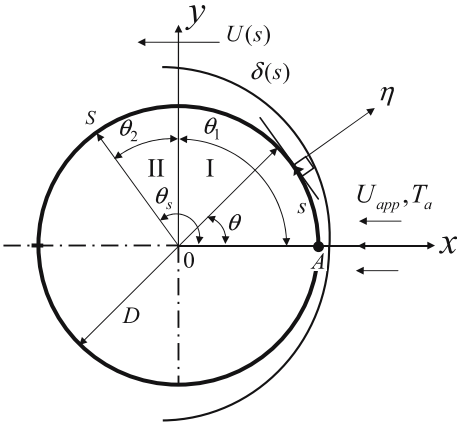

Fig. 1 Flow over circular cylinder

approximated by a fourth-order polynomial as suggested by Pohlhausen [8]:

$$\frac{u}{U(s)} = (2\eta_H - 2\eta_H^3 + \eta_H^4) + \frac{\lambda}{6}(\eta_H - 3\eta_H^2 + 3\eta_H^3 - \eta_H^4) \tag{4}$$

where $\eta_H = \eta/\delta(s)$ is the dimensionless distance normal to the cylinder surface in the hydrodynamic boundary layer, $U(s) = 2U_{app}\sin\theta$ is the potential flow velocity outside the boundary layer, and λ is the pressure gradient parameter, given by

$$\lambda = \frac{\delta^2}{v}\frac{dU(s)}{ds} \tag{5}$$

With the help of velocity profiles, Schlichting [9] showed that the parameter λ is restricted to the range $-12 \le \lambda \le 12$. Khan [7] solved momentum integral equation using Von Karman-Pohlhausen method and obtained λ values corresponding to each position along the cylinder surface. These values were fitted by the least squares method into two separate polynomials, that is, for region I

$$\lambda_1 = 7.239\sum_{j=0}^{7} a_j\theta^j \tag{6}$$

and for region II

$$\lambda_2 = 0.3259\sum_{j=0}^{10} b_j\theta^j \tag{7}$$

where a_j and b_j are the coefficients given in tabular form [7]. These polynomials are used to determine the heat transfer coefficients in both regions.

5 Temperature distribution

For both the viscous and inviscid flow models, the temperature distribution in the thermal boundary layer can be approximated by a third-order polynomial

$$\frac{T - T_a}{T_w - T_a} = A + B\eta_T + C\eta_T^2 + D\eta_T^3 \tag{8}$$

where $\eta_T = \eta/\delta_T\ (s)$ is the dimensionless distance normal to the cylinder surface in the thermal boundary layer. Using the thermal boundary conditions, the temperature distribution will be

$$\frac{T - T_a}{T_w - T_a} = 1 - \frac{3}{2}\eta_T + \frac{1}{2}\eta_T^3 \tag{9}$$

for the isothermal boundary condition and

$$T - T_a = \frac{2q\delta_T}{3k_f}\left(1 - \frac{3}{2}\eta_T + \frac{1}{2}\eta_T^3\right) \tag{10}$$

for the isoflux boundary condition.

6 Heat transfer

The main parameter of interest in this study is the dimensionless average heat transfer coefficient, Nu_D for small Prandtl numbers (0.004–0.03). This parameter is determined by integrating Eq. (1) from the cylinder surface to the thermal boundary layer edge, which will be solved for both the viscous and inviscid flow models under different thermal boundary conditions.

6.1 Inviscid model

In liquid metals the thickness of the viscous boundary layer is small compared with that of the thermal boundary layer and may be ignored, so that the fluid flow can be considered as a potential flow of an ideal fluid. Assuming the presence of a thin thermal boundary layer δ_T along the cylinder surface, the energy integral equation for the isothermal boundary condition can be written as

$$\frac{d}{ds}\int_0^{\delta_T}(T - T_a)u\,d\eta = -\alpha\left.\frac{\partial T}{\partial\eta}\right|_{\eta=0} \tag{11}$$

Using the potential flow velocity and temperature profiles, and assuming $\xi = \delta/\delta_T \ll 1$, Eq. (11) can be simplified to

$$\delta_T\frac{d}{ds}[U(s)\delta_T] = 4\alpha \tag{12}$$

Multiplying both sides of Eq. (12) by $U(s)$ and integrating with respect to s, one can obtain the local dimensionless thermal boundary layer thickness:

$$\frac{\delta_T(\theta)}{D} = \frac{1}{\sqrt{Pe_D}}\sqrt{\frac{2}{1+\cos\theta}} \tag{13}$$

where $Pe_D = \alpha/(U_{app}\ D)$ is the Peclet number. For the isothermal boundary condition, the local heat transfer coefficient is

$$h(\theta) = -\frac{k_f\left.\frac{\partial T}{\partial\eta}\right|_{\eta=0}}{T_w - T_a} = \frac{3k_f}{2D}\sqrt{\frac{1+\cos\theta}{2}}Pe_D^{1/2} \tag{14}$$

Thus, the local Nusselt number will be

$$\left.\frac{Nu_D(\theta)}{Pe_D^{1/2}}\right|_{\text{isothermal}} = 1.061\sqrt{1+\cos\theta} \tag{15}$$

The average heat transfer coefficient is defined as

$$h = \frac{1}{\pi}\int_0^{\pi} h(\theta)d\theta = 0.95\frac{k_f}{D}Pe_D^{1/2} \tag{16}$$

Therefore, the average Nusselt number of an isothermal cylinder will be

$$\frac{Nu_D|_{\text{isothermal}}}{Pe_D^{1/2}} = 0.95 \tag{17}$$

which is 6% less than the inviscid flow model of Grosh and Cess [3]. For the isoflux boundary condition, the energy integral equation can be written as

$$\frac{\mathrm{d}}{\mathrm{d}x}\int_0^{\delta_T}(T - T_a)u\mathrm{d}\eta = \frac{q}{\rho c_p} \tag{18}$$

Using the potential flow velocity and temperature profile for the isoflux boundary condition and assuming constant heat flux and thermophysical properties, Eq. (18) can be simplified to

$$\frac{\mathrm{d}}{\mathrm{d}s}\left[U(s)\delta_T^2\right] = \frac{4v}{Pr} \tag{19}$$

Integrating both sides with respect to s and simplifying, one can get:

$$\frac{\delta_T(\theta)}{D} = \frac{1}{\sqrt{Pe_D}}\sqrt{\frac{\theta}{\sin\theta}} \tag{20}$$

The local temperature difference will be:

$$\Delta T(\theta) = \frac{2q}{3k_f}\delta_T = \frac{2q}{3k_f}\frac{D}{Pe_D^{1/2}}\sqrt{\frac{\theta}{\sin\theta}} \tag{21}$$

Therefore, the local heat transfer coefficient and Nusselt number will be

$$h(\theta) = \frac{3k_f}{2D}\sqrt{\frac{\sin\theta}{\theta}}Pe_D^{1/2} \tag{22}$$

$$Nu_D(\theta) = 1.5\sqrt{\frac{\sin\theta}{\theta}}Pe_D^{1/2} \tag{23}$$

Following the same procedure for the average heat transfer coefficient as mentioned previously, one can obtain the average Nusselt number for an isoflux cylinder as

$$\frac{Nu_D|_{\text{isoflux}}}{Pe_D^{1/2}} = 1.09 \tag{24}$$

This Nusselt number is 6% greater than the average Nusselt number for an isothermal circular cylinder, Eq. (17). Combining the results for both thermal boundary conditions, the heat transfer parameter for the inviscid flow model can be written as

$$\frac{Nu_D}{Pe_D^{1/2}} = \begin{cases} 0.95 & \text{UWT} \\ 1.09 & \text{UWF} \end{cases} \tag{25}$$

6.2 Viscous flow model

In this model, the velocity distribution inside the hydrodynamic boundary layer is approximated as a fourth-order polynomial, Eq. (4), whereas the potential flow velocity is used outside the boundary layer. Using the temperature distribution, Eq. (9), for isothermal boundary condition, the energy integral equation is written as

$$\frac{\mathrm{d}}{\mathrm{d}s}\left\{\delta_T\int_0^1 f(\eta_T)u\mathrm{d}\eta_T\right\} = \frac{3\alpha}{2\delta_T} \tag{26}$$

where

$$f(\eta_T) = 1 - \frac{3}{2}\eta_T + \frac{1}{2}\eta_T^3 \tag{27}$$

When $\delta/\ \delta_T = \zeta \ll 1$, the integral in Eq. (26) can be divided into two parts:

$$\frac{\mathrm{d}}{\mathrm{d}s}\left\{\delta_T\left[\int_0^{\zeta} f(\eta_T)u\mathrm{d}\eta_T + \int_{\zeta}^1 f(\eta_T)u\mathrm{d}\eta_T\right]\right\} = \frac{3\alpha}{2\delta_T} \tag{28}$$

or

$$\delta_T\frac{\mathrm{d}}{\mathrm{d}s}\{\delta_T(I_1 + I_2)\} = \frac{3\alpha}{2} \tag{29}$$

where

$$I_1 = U(s)\int_0^{\zeta} f(\eta_T)f(\eta_H)\mathrm{d}\eta_T = \frac{\zeta U(s)}{10}\left(7 + \frac{\lambda}{12}\right) \tag{30}$$

$$I_2 = \int_{\zeta}^1 U(s)f(\eta_T)\mathrm{d}\eta_T = U(s)\left(\frac{3}{8} - \zeta\right) \tag{31}$$

substituting these values in Eq. (29), and simplifying, we get

$$\delta_T\frac{\mathrm{d}}{\mathrm{d}s}\left\{U(s)\delta_T\left(\frac{3}{8} - \frac{3\zeta}{10} + \frac{\zeta\lambda}{120}\right)\right\} = \frac{3\alpha}{2} \tag{32}$$

This equation can be rewritten separately for the two regions (Fig. 1)

$$\delta_T\frac{\mathrm{d}}{\mathrm{d}s}\left\{U(s)\delta_T\left(\frac{3}{8} - \frac{3\zeta}{10} + \frac{\zeta\lambda_1}{120}\right)\right\} = \frac{3\alpha}{2} \tag{33}$$

for region I, and

$$\delta_T\frac{\mathrm{d}}{\mathrm{d}s}\left\{U(s)\delta_T\left(\frac{3}{8} - \frac{3\zeta}{10} + \frac{\zeta\lambda_2}{120}\right)\right\} = \frac{3\alpha}{2} \tag{34}$$

for region II. Multiplying both sides of Eq. (33) by $U(s)\left(\frac{3}{8} - \frac{3\zeta}{10} + \frac{\zeta\lambda_1}{120}\right)$ and integrating in region I, from $0 \le \theta \le \theta_1$ and simplifying, we get

$$\left\{U(s)\delta_{T_1}\left(\frac{3}{8} - \frac{3\zeta}{10} + \frac{\zeta\lambda_1}{120}\right)\right\}^2 = 3D\alpha U_{\text{app}}I_3 \tag{35}$$

where

$$I_3 = \int_0^{\theta} \sin\theta\left(\frac{3}{8} - \frac{3\zeta}{10} + \frac{\zeta\lambda_1}{120}\right)\mathrm{d}\theta \tag{36}$$

Neglecting higher powers of ζ and simplifying Eq. (35), we get

$$\Delta_1^2 - \frac{1}{45}(36-\lambda_1)\sqrt{\frac{\lambda_1 Pr}{\cos\theta}}\Delta_1 - \frac{2}{1+\cos\theta} = 0 \tag{37}$$

which is a quadratic equation in Δ_1, where

$$\Delta_1 = \frac{\delta_{T_1}}{D}\sqrt{Pe_D} \tag{38}$$

Solving Eq. (37), we get

$$\begin{aligned}\Delta_1 &= \frac{1}{90}(36-\lambda_1)\sqrt{\frac{\lambda_1 Pr}{\cos\theta}} \\ &\quad + \frac{1}{90}\sqrt{(36-\lambda_1)^2\frac{\lambda_1 Pr}{\cos\theta} + \frac{360}{1+\cos\theta}} \\ &= f_1(\theta, Pr)\end{aligned} \tag{39}$$

The local heat transfer coefficient is given by

$$h_1(\theta) = \frac{3k_f}{2\delta_{T_1}} = \frac{3k_f}{2D}\cdot\frac{\sqrt{Pe_D}}{f_1(\theta, Pr)} \tag{40}$$

Therefore local Nusselt number in region I will be

$$Nu_{D1}(\theta) = \frac{3}{2}\cdot\frac{\sqrt{Pe_D}}{f_1(\theta, Pr)} \tag{41}$$

Similarly multiplying Eq. (34) by $U(s)\left(\frac{3}{8} - \frac{3\zeta}{10} + \frac{\zeta\lambda_2}{120}\right)$ and simplifying in the same way as before, we get

$$\Delta_2^2 - \frac{1}{45}(36-\lambda_2)\sqrt{\frac{\lambda_2 Pr}{\cos\theta}}\Delta_2 - \frac{2(3-2\cos\theta)}{3\sin\theta^2} = 0 \tag{42}$$

which is a quadratic equation in Δ_2, where

$$\Delta_2 = \frac{\delta_{T_2}}{D}\sqrt{Pe_D} \tag{43}$$

Solving Eq. (42), we get

$$\begin{aligned}\Delta_2 &= \frac{1}{90}(36-\lambda_2)\sqrt{\frac{\lambda_2 Pr}{\cos\theta}} \\ &\quad + \frac{1}{90}\sqrt{(36-\lambda_2)^2\frac{\lambda_2 Pr}{\cos\theta} + \frac{120(3-2\cos\theta)}{\sin^2\theta}} \\ &= f_2(\theta, Pr)\end{aligned} \tag{44}$$

The local heat transfer coefficient is given by

$$h_2(\theta) = \frac{3k_f}{2\delta_{T_2}} = \frac{3k_f}{2D}\cdot\frac{\sqrt{Pe_D}}{f_2(\theta, Pr)} \tag{45}$$

The local Nusselt number in region II will be

$$Nu_{D2}(\theta) = \frac{3}{2}\cdot\frac{\sqrt{Pe_D}}{f_2(\theta, Pr)} \tag{46}$$

Thus the local Nusselt number from front stagnation point to the separation point will be

$$\begin{aligned}Nu_D(\theta) &= Nu_{D2}(\theta) + Nu_{D2}(\theta) \\ &= \frac{3}{2}\left\{\frac{1}{f_1(\theta, Pr)} + \frac{1}{f_2(\theta, Pr)}\right\}\cdot\sqrt{Pe_D}\end{aligned} \tag{47}$$

The average heat transfer coefficient is defined as

$$h = \frac{1}{\pi}\int_0^{\pi} h(\theta)\mathrm{d}\theta = \frac{1}{\pi}\left\{\int_0^{\theta_s} h(\theta)\mathrm{d}\theta + \int_{\theta_s}^{\pi} h(\theta)\mathrm{d}\theta\right\} \tag{48}$$

The integral analysis is unable to predict heat transfer values from the separation point to the rear stagnation point. Experimental studies of Andreevskii [3] and Ishiguro et al. [4] show that the local Nusselt number decreases monotonically from the front stagnation point to the rear stagnation point, whereas numerical studies of Sugiyama and Ishiguro [5] show that the local Nusselt numbers have almost constant values behind the cylinder. However, experiments of Sugiyama and Ishiguro [5] show that the local Nusselt numbers increase after the separation due to the flow induced in the separation region at high Reynolds numbers. From a collection of all known data for large Prandtl numbers, Van der Hegge Zijnen [10] demonstrated that the heat transferred from the rear portion of the cylinder can be determined from $Nu_D = 0.001\ Re_D$ that shows the weak dependence of average heat transfer from the rear portion of the cylinder on Reynolds numbers. In order to include the share of heat transfer from the rear portion of the cylinder, the local heat transfer coefficients are integrated upto the separation point and averaged over the whole surface, that is

$$\begin{aligned}h &= \frac{1}{\pi}\int_0^{\theta_s} h(\theta)\mathrm{d}\theta \\ &= \frac{1}{\pi}\left\{\int_0^{\theta_1} h_1(\theta)\mathrm{d}\theta + \int_{\theta_1}^{\theta_s} h_2(\theta)\mathrm{d}\theta\right\} \\ &= \frac{1}{\pi}\frac{3k_f}{2D}\left\{\int_0^{\theta_1}\frac{1}{f_1(\theta, Pr)}(\theta)\mathrm{d}\theta + \int_{\theta_1}^{\theta_s}\frac{1}{f_2(\theta, Pr)}(\theta)\mathrm{d}\theta\right\}\sqrt{Pe_D}\end{aligned} \tag{49}$$

Equation (49) is solved for different Prandtl numbers (0.004–0.03) and the results are fitted to a correlation in terms of Prandtl number. The average Nusselt number for the isothermal cylinder can be written as:

$$Nu_D|_{\text{isothermal}} = \frac{0.465}{(Pr+0.0077)^{0.1}}\cdot Pe_D^{1/2} \tag{50}$$

For isoflux thermal boundary condition, Eq. (18) can be solved using Eqs. (4) and (10) and following the same

procedure as for isothermal case. The simplified result can be written as:

$$\frac{\mathrm{d}}{\mathrm{d}s}\left\{U(s)\delta_{\mathrm{T}}^2\left(\frac{3}{8}-\frac{3\zeta}{10}+\frac{\zeta\lambda}{120}\right)\right\}=\frac{3\nu}{2Pr} \tag{51}$$

Rewriting Eq. (51) in the same way as Eqs. (33) and (34), and simplifying, we get the following quadratic equations:

$$\Delta_1^2-\frac{1}{90}(36-\lambda_1)\sqrt{\frac{\lambda_1 Pr}{\cos\theta}}\Delta_1-\frac{\theta}{\sin\theta}=0 \tag{52}$$

$$\Delta_2^2-\frac{1}{90}(36-\lambda_2)\sqrt{\frac{\lambda_2 Pr}{\cos\theta}}\Delta_2-\frac{(2\theta-\pi/2)}{\sin\theta}=0 \tag{53}$$

The solution of these quadratic equations give

$$\begin{aligned}\Delta_1&=\frac{1}{180}(36-\lambda_1)\sqrt{\frac{\lambda_1 Pr}{\cos\theta}}\\&\quad+\frac{1}{180}\sqrt{(36-\lambda_1)^2\frac{\lambda_1 Pr}{\cos\theta}+\frac{32400\theta}{\sin\theta}}\\&=f_3(\theta,Pr)\end{aligned} \tag{54}$$

$$\begin{aligned}\Delta_2&=\frac{1}{180}(\lambda_2-36)\sqrt{\frac{\lambda_2 Pr}{\cos\theta}}\\&\quad+\frac{1}{180}\sqrt{(36-\lambda_2)^2\frac{\lambda_2 Pr}{\cos\theta}+\frac{16200(\pi-4\theta)}{\sin^2\theta}}\\&=f_4(\theta,Pr)\end{aligned} \tag{55}$$

Using these dimensionless thermal boundary layer thicknesses, local surface temperatures for the two regions can be obtained from temperature distribution

$$\begin{aligned}\Delta T_1(\theta)&=\frac{2q\delta_{\mathrm{T}_1}}{3k_{\mathrm{f}}}\\\Delta T_2(\theta)&=\frac{2q\delta_{\mathrm{T}_2}}{3k_{\mathrm{f}}}\end{aligned} \tag{56}$$

The local heat transfer coefficient can now be obtained from its definition as

$$h_1(\theta)=\frac{q}{\Delta T_1(\theta)}\ \text{and}\ h_2(\theta)=\frac{q}{\Delta T_2(\theta)} \tag{57}$$

which give the local Nusselt numbers for the cross flow over a cylinder with constant flux. Integrating local heat transfer coefficients over the circumference of the cylinder, we get the average Nusselt numbers for different Prandtl numbers. The results are fitted again into a single correlation in terms of Prandtl number. Therefore, average Nusselt number for an isoflux cylinder can be written as

$$Nu_D|_{\text{isoflux}}=\frac{0.645}{(Pr+0.0077)^{0.04}}\cdot Pe_D^{1/2} \tag{58}$$

Combining the results for both thermal boundary conditions, the heat transfer parameter for the viscous flow model can be written as

$$\frac{Nu_D}{P_D^{1/2}}=\begin{cases}\dfrac{0.465}{(Pr+0.0077)^{0.1}} & \text{UWT}\\[2ex]\dfrac{0.645}{(Pr+0.0077)^{0.04}} & \text{UWF}\end{cases} \tag{59}$$

7 Results and discussion

The local heat transfer parameter $Nu_D\ (\theta)/Pe_D^{1/2}$ is plotted in Fig. 2 for viscous flow model under an isoflux thermal boundary condition. It is compared with available experimental/numerical data for different Pe_D numbers and also with the inviscid flow model of Grosh and Cess [1]. The present viscous flow model is found to be in good agreement with the existing experimental data of Ishiguro et al. [6] and also with numerical data of Sugiyama and Ishiguro [5]. However, the results of Grosh and Cess [1] are higher for the same thermal boundary condition.

Figure 3 shows the present average Nusselt numbers versus Pe_D for the inviscid flow models under both thermal boundary conditions. They are compared with the models of Grosh and Cess [1] for the same thermal boundary conditions. It is found that the results of Grosh and Cess [1] are 6% higher for isothermal and 29% higher for isoflux thermal boundary conditions. The average heat transfer coefficients obtained from the present inviscid flow model versus Pe_D are plotted in Fig. 4. They are compared with the available experimental data of Andreevskii [3] and Ishiguro et al. [6] and also with the present and the inviscid flow models of Grosh and Cess [1]. It is observed that all inviscid flow models give higher heat transfer coefficients whereas the

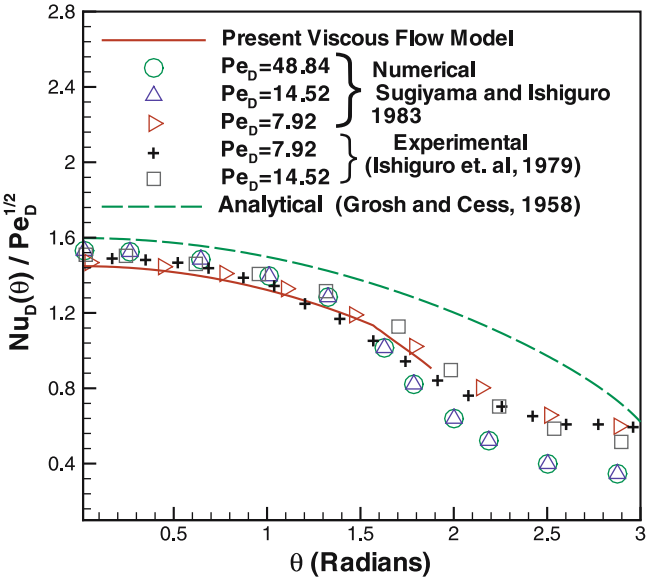

Fig. 2 Comparison of local nusselt numbers for isoflux cylinder

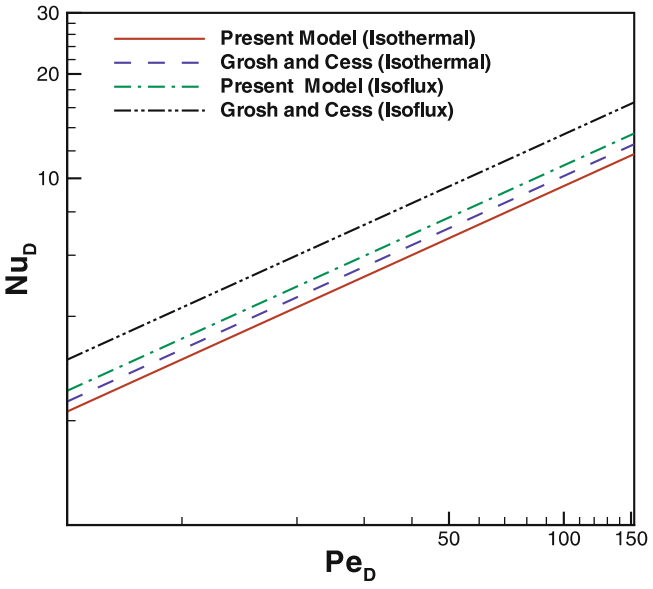

Fig. 3 Comparison of inviscid flow models for isothermal and isoflux thermal boundary conditions

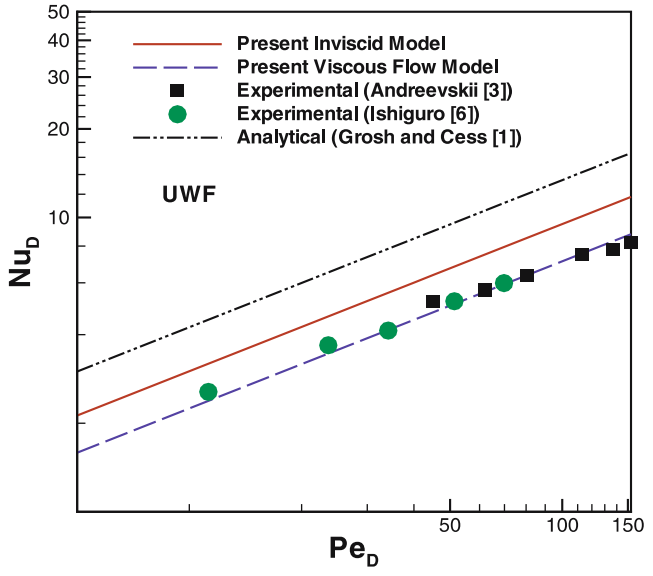

Fig. 4 Average heat transfer in crossflow of liquid metal around single cylinder

viscous flow model is in good agreement with the available experimental/numerical data. This is due to neglecting hydrodynamic boundary layer compared with the thermal boundary layer and the effect of the separation of flow in the inviscid flow models.

8 Summary and conclusions

Two separate viscous and inviscid flow models are developed for average heat transfer to liquid metals from a single circular cylinder in cross-flow. The inviscid flow model gives higher local and average heat transfer coefficients, whereas the viscous flow model gives results in agreement with the available experimental/numerical data. From the comparisons of the local and average heat transfer coefficients, it is confirmed that the disagreement between the inviscid and viscous flow models originated with the neglect of the hydrodynamic boundary layer compared with the thermal boundary layer and the effect of the separation of flow on heat transfer. It was also confirmed from the comparison with the experimental/numerical results that the heat transfer characteristics of liquid metal in cross-flow around a single cylinder can be accurately predicted with the present viscous flow model.

Acknowledgments The authors gratefully acknowledge the financial support of Natural Sciences and Engineering Research Council of Canada and the Center for Microelectronics Assembly and Packaging.

References

1. Grosh RJ, Cess RD (1958) Heat transfer to fluids with low prandtl numbers for flow across plates and cylinders of various cross sections. ASME Trans 80(3):667–676
2. Cess RD, Grosh RJ (1958) Heat transmission to fluids with low prandtl numbers for flow through tube banks. ASME Trans 80(3):677–682
3. Andreevskii AA (1959) Heat transfer in transverse flow of molten sodium around a single cylinder. Sov J At Energy 7:745–747
4. Ishiguro R, Kumada T, Sugiyama K, Ikezaki E (1976) Experimental study of heat transfer around a circular cylinder in a liquid sodium cross flow. Int Chem Eng 16(2):249–253
5. Sugiyama K, Ishiguro R (1978) Numerical study of local heat transfer around a circular cylinder in a liquid sodium cross flow. Heat Transf Jpn Res 7(4):59–68
6. Ishiguro R, Sugiyama K, Kumada T (1979) Heat transfer across a circular cylinder in a liquid sodium cross flow. Int J Heat Mass Transf 22(7):1041–1048
7. Khan WA (2004) Modeling of fluid flow and heat transfer for optimization of pin-fin heat sinks. PhD Thesis, Department of Mechanical Engineering, University of Waterloo
8. Pohlhausen K (1921) Zur Näherungsweise Integration der Differential Gleichung der Laminaren Reibungschicht. Zeitschrift für angewandte Mathematic und Mechanic 1:252–268
9. Schlichting H (1979) Boundary layer theory, 7th edn. McGraw-Hill, New York
10. Van der Hegge Zijnen BG (1956) Modified correlation formulae for heat transfer by natural and forced convection from horizontal cylinders. Appl Sci Res A 6(2–3):129–140